SUPPORTING INFORMATION

Intermolecular Interactions of A-Site Cations Modulate Stability of 2D Metal-Halide Perovskites

Edoardo Mosconi,[1,2*] Asma A. Alothman,[2] Run Long,[3] Waldemar Kaiser,[1,*] Filippo De Angelis[1,4]

[1]*Computational Laboratory for Hybrid/Organic Photovoltaics (CLHYO), Istituto CNR di Scienze e Tecnologie Chimiche "Giulio Natta" (CNR-SCITEC), Via Elce di Sotto 8, 06123 Perugia, Italy.*

[2] *Chemistry Department, College of Science, King Saud University, Riyadh 11451, Kingdom of Saudi Arabia.*

[3]*College of Chemistry, Key Laboratory of Theoretical & Computational Photochemistry of Ministry of Education, Beijing Normal University, Beijing 100875, People's Republic of China.*

[4]*Department of Chemistry, Biology and Biotechnology, University of Perugia and UdR INSTM, Via Elce di Sotto 8, 06123 Perugia, Italy.*

Corresponding Author

e-Mail: waldemar.kaiser@scitec.cnr.it ; edoardo.mosconi@cnr.it ;

Computational Details

DFT calculations. Density functional theory (DFT) calculations were carried out within the Quantum Espresso software package.[1] We employed the PBE functional[2] with scalar relativistic ultrasoft pseudopotentials,[3] with valence electrons from 2s, 2p for O, N, and C; 1s for H; 5s, and 5p for I; 6s, 6p, and 5d for Pb; 3s, 3p for S. Plane-wave basis set cutoffs for the smooth part of the wave functions and the augmented density were set to 25 and 200 Ry, respectively. Starting from the experimental XRD structures (NBT_2PbI_4 from ref. 4; $MTEA_2PbI_4$ derived from ref. 5 (CIF can be found as supplementary document); PEA_2PbI_4 from ref. 6; I-PMA_2PbI_4 from ref. 7; ABA_2PbI_4 from ref. 8), geometry optimization has been carried out with fixed cell parameters and followed by single point calculations for including Grimme D3 dispersion corrections.[9] A k-point grid 4×4×1 was used with 4 points along the two short periodic directions and 1 point along the long stacking direction. The PMA_2PbI_4* structure was generated starting from the optimized I-PMA_2PbI_4 geometry, replacing the I atoms of the aromatic ring with H and subsequent relaxation while keeping cell parameter and all atom positions expected the replaced H fixed in order to understand the explicit role of halogen at exactly the same geometry.

Decomposition of passivation energy. The total passivation energy (ΔE_{Tot}) was decomposed into intermolecular and adsorption contributions ΔE_{Aggr} and ΔE_{Ads}, respectively. ΔE_{Aggr} gives the intermolecular interaction energy associated with the formation of the organic layer; ΔE_{Ads} represents the interaction energy between the organic and the inorganic layer.

The total passivation energy (ΔE_{Tot}) is calculated following

$$\Delta E_{Tot} = [E_{bulk} - (E_{cut} + 4\times E_{mol})]/4$$

where E_{bulk} is the total energy of the perovskite supercell, E_{cut} is the total energy of the supercell after removal of one organic layer, and E_{mol} is the energy of AI (A=NBT, MTEA, PEA, I-PMA, PMA, ABA) as a single salt molecule. Please refer to Figure S1. We normalize ΔE_{Tot} by the number of organic molecules, *i.e.* 4 in our case, which also correspond to the number of the undercoordinated Pb atoms on the remaining slab.

The aggregation energy (ΔE_{Aggr}) is calculated as follows:

$$\Delta E_{Aggr} = (E_{layer} - 4\times E_{mol})/4$$

where E_{layer} is the single point energy of one organic layer that has been taken from the perovskite supercell. Note that E_{layer} is normalized by the number of organic salt molecules, *i.e.* 4, within the organic layer.

ΔE_{Ads} is calculated directly as the difference between ΔE_{Tot} and ΔE_{Aggr}:

$$\Delta E_{Ads} = \Delta E_{Tot} - \Delta E_{Aggr}$$

ΔE_{Layer} is the interaction energy between 1/2Layer1 and 1/2Layer2, see Figure S1, normalized by the number of organic molecules:

$$\Delta E_{Layer} = (E_{layer} - E_{1/2Layer1} - E_{1/2Layer2})/4$$

Finally, ΔE_{Inter} is the intermolecular interaction in the $E_{1/2layer1}$ per organic molecule:

$$\Delta E_{Inter} = E_{1/2Layer1} - 2 \times E_{mol}$$

To clearly describe the structure associated to E_{bulk}, E_{cut}, E_{layer}, $E_{1/2Layer1}$, $E_{1/2Layer2}$ we refer to Figure S1. All calculated quantities are reported in Table S1.

Table S1. Decomposition of the chemical interaction in 2D metal-halide perovskites. Interaction energies are calculated in eV with and without including DFT-D3 dispersion contribution. The difference between the values calculated with and without D3 are also reported.

		ΔE_{Tot}	ΔE_{Aggr}	ΔE_{Ads}	ΔE_{Layer}	ΔE_{Inter}
NBT_2PbI_4	w/o D3	-1.82	-1.16	-0.66	0.03	-1.19
	D3	**-2.63**	**-1.56**	**-1.08**	**-0.12**	**-1.43**
	Diff.	*-0.81*	*-0.40*	*-0.42*	*-0.15*	*-0.24*
$MTEA_2PbI_4$	w/o D3	-1.62	-1.06	-0.56	0.04	-1.10
	D3	**-2.60**	**-1.60**	**-1.00**	**-0.21**	**-1.38**
	Diff.	*-0.97*	*-0.54*	*-0.44*	*-0.25*	*-0.28*
PEA_2PbI_4	w/o D3	-1.95	-1.28	-0.67	0.03	-1.31
	D3	**-2.96**	**-1.85**	**-1.11**	**-0.14**	**-1.71**
	Diff.	*-1.01*	*-0.57*	*-0.43*	*-0.16*	*-0.41*
I-PMA_2Pb_I4	w/o D3	-1.76	-1.12	-0.64	0.04	-1.16
	D3	**-2.93**	**-1.84**	**-1.10**	**-0.30**	**-1.53**
	Diff.	*-1.18*	*-0.72*	*-0.46*	*-0.35*	*-0.37*
PMA_2PbI_4*	w/o D3	-1.79	-1.13	-0.66	-0.01	-1.12
	D3	**-2.65**	**-1.56**	**-1.10**	**-0.11**	**-1.44**
	Diff.	*-0.87*	*-0.43*	*-0.44*	*-0.10*	*-0.33*
ABA_2PbI_4	w/o D3	-2.85	-2.06	-0.79	-0.80	-1.26
	D3	**-3.90**	**-2.65**	**-1.24**	**-1.10**	**-1.55**
	Diff.	*-1.05*	*-0.60*	*-0.45*	*-0.31*	*-0.29*

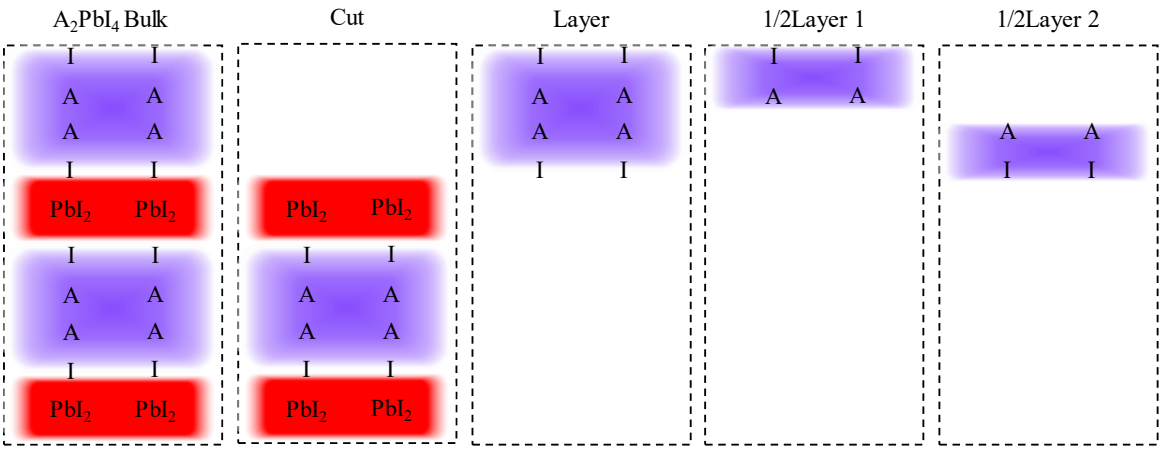

Figure S1. Schematic representation of the structural decomposition for the evaluation of the interaction energies.

To verify the absence of artificial electrostatic interactions upon cutting the perovskite slabs, we investigate the planar averaged electrostatic potential along the plane stacking direction for the A_2PbI_4 bulk, as well as the Cut and Layer constituents in the structural decomposition process, see Figure S1. In Figure S2, we visualize the electrostatic potential for PEA_2PbI_4 and ABA_2PbI_4. The electrostatic potential of the constituents follows the ones of the bulk and, most importantly, remains completely flat in the removed regions. Thus, we may rule out the presence of artificial electrostatic interactions in the structural decomposition.

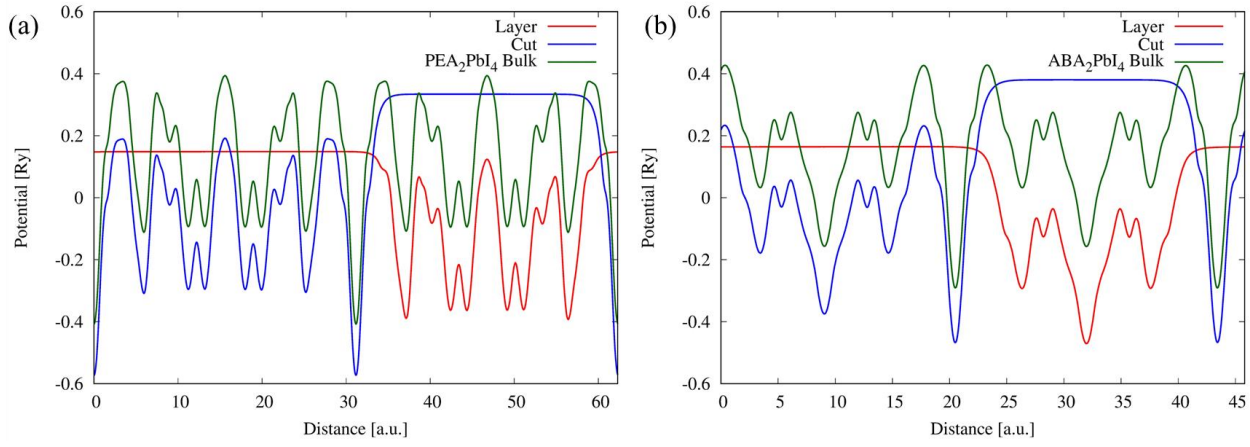

Figure S2. Planar electrostatic potential, averaged along the plane stacking direction, for (a) PEA_2PbI_4 and (b) ABA_2PbI_4. In blue and red color, the electrostatic potential of the Cut and Layer constituents are visualized.

Validation of interaction energies for non-local exchange correlation functionals. To understand potential limitations when using the semilocal PBE functional plus D3 dispersion interactions, we calculate each interaction energy using the non-local exchange-correlation functional optB88-vdW[10-13] for PEA_2PbI_4 and ABA_2PbI_4 as two of our examples using the optB88-vdW functional within the Quantum Espresso software package. We observe a comparable change in ΔE_{Tot} when using the optB88-vdW of 0.32 eV for PEA and of 0.38 eV for ABA with respect to the PBE+D3 values, see Table S2. The change in ΔE_{Tot} is evenly distributed between ΔE_{Aggr} and ΔE_{Ads}. Consequently, trends predicted from PBE+D3 calculations hold also when employing more advanced models, while the absolute values of interaction energies increase equally for all considered cations.

Table S2. Decomposition of the chemical interaction in 2D metal-halide perovskites for A = PEA and ABA. Interaction energies are calculated in eV using the PBE+D3 and the non-local optB88-vdW exchange correlation functional. The difference between the values calculated with PBE+D3 and optB88-vdW are also reported.

		ΔE_{Tot}	ΔE_{Aggr}	ΔE_{Ads}	ΔE_{Layer}	ΔE_{Inter}
PEA_2PbI_4	PBE+D3	-2.96	-1.85	-1.11	-0.14	-1.71
	optB88-vdW	-3.28	-2.00	-1.28	-0.22	-1.78
	Diff.	*-0.32*	*-0.15*	*-0.17*	*-0.08*	*-0.07*
ABA_2PbI_4	PBE+D3	-3.90	-2.65	-1.24	-1.10	-1.55
	optB88-vdW	-4.28	-2.85	-1.42	-1.23	-1.62
	Diff.	*-0.38*	*-0.20*	*-0.18*	*-0.13*	*-0.07*

Solvation free energies. To evaluate the cation solvation free energies (ΔG_{solv}) reported in Table 1, we carried out with Gaussian09 program package.[14] The geometry optimization in water (G_{solv}) using the C-PCM model,[15] followed by a single point in vacuo (G_{vac}). The ΔG_{solv} is calculated as a difference between $G_{solv} - G_{vac}$. These quantities are calculated employing B3LYP functional[16] along with 6-31g* basis set and, only for I species in I-PMA^+, we used lanl2dz[17] and related lanl2 pseudo potential.

References

(1) Giannozzi, P.; Baroni, S.; Bonini, N.; Calandra, M.; Car, R.; Cavazzoni, C.; Ceresoli, D.; Chiarotti, G. L.; Cococcioni, M.; Dabo, I.*; et al.* QUANTUM ESPRESSO: A Modular and Open-Source Software Project for Quantum Simulations of Materials. *J. Phys. Condens. Matter* **2009**, *21*, 395502.

(2) Perdew, J. P.; Burke, K.; Ernzerhof, M. Generalized Gradient Approximation Made Simple. *Phys. Rev. Lett.* **1996**, *77*, 3865–3868.

(3) Vanderbilt, D. Soft self-consistent pseudopotentials in a generalized eigenvalue formalism. *Phys. Rev. B.* **1990**, *41*, 7892(R)

(4) Billing, D. G.; Lemmerer, A. Synthesis, characterization and phase transitions in the inorganic-organic layered perovskite-type hybrids $(C_nH_{2n+1}NH_3)_2PbI_4$, n = 4, 5 and 6. *Acta Crystallogr., Sect. B, Struct. Sci.* **2007**, *63*, 735–747.

(5) Ren, H.; Yu, S.; Chao, L.; Xia, Y.; Sun, Y.; Zuo, S.; Li, F.; Niu, T.; Yang, Y.; Ju, H.*; et al.* Efficient and stable Ruddlesden–Popper perovskite solar cell with tailored interlayer molecular interaction. *Nat. Photonics* **2020**, *14*, 154–163.

(6) Du, K.-Z.; Tu, Q.; Zhang, X.; Han, Q.; Liu, J.; Zauscher, S.; Mitzi, D. B. Two-Dimensional Lead(II) Halide-Based Hybrid Perovskites Templated by Acene Alkylamines: Crystal Structures, Optical Properties, and Piezoelectricity. *Inorg. Chem.* **2017**, *56*, 9291–9302.

(7) Tremblay, M.-H.; Bacsa, J.; Zhao, B.; Pulvirenti, F.; Barlow, S.; Marder, S. R. Structures of (4-Y-$C_6H_4CH_2NH_3)_2PbI_4$ {Y = H, F, Cl, Br, I}: Tuning of Hybrid Organic Inorganic Perovskite Structures from Ruddlesden–Popper to Dion–Jacobson Limits. *Chem. Mater.* **2019**, *31*, 6145–6153.

(8) Mercier, N. $(HO_2C(CH_2)_3NH_3)_2(CH_3NH_3)Pb_2I_7$: a predicted non-centrosymmetrical structure built up from carboxylic acid supramolecular synthons and bilayer perovskite sheets. *CrystEngComm* **2005**, *7*, 429.

(9) Grimme, S.; Antony, J.; Ehrlich, S.; Krieg, H. A Consistent and Accurate *Ab Initio* Parametrization of Density Functional Dispersion Correction (DFT-D) for the 94 Elements H-Pu. *J. Chem. Phys.* **2010**, *132*, 154104.

(10) Thonhauser, T.; Zuluaga, S.; Arter, C. A.; Berland, K.; Schröder, E.; and Hyldgaard, P. Spin Signatures of Nonlocal Correlation Binding in Metal-Organic Frameworks. *Phys. Rev. Lett.* **2015**, *115*, 136402.

(11) Thonhauser, T.; Cooper, V.R.; Li, S.; Puzder, A.; Hyldgaard, P.; Langreth, D.C. Van der Waals density functional: Self-consistent potential and the nature of the van der Waals bond. *Phys. Rev. B* **2007**, *76*, 125112.

(12) Berland, K.; Cooper, V.R.; Lee, K.; Schröder, E.; Thonhauser, T.; Hyldgaard, P.; Lundqvist, B.I. van der Waals forces in density functional theory: a review of the vdW-DF method. *Rep. Prog. Phys.* **2015**, *78*, 066501.

(13) Langreth, D.C.; Lundqvist, B.I.; Chakarova-Käck, S.D.; Cooper, V.R.; Dion, M.; Hyldgaard, P.; Kelkkanen, A.; Kleis, J.; Kong, L.; Li, S.; et al. A density functional for sparse matter. *J. Phys.: Condens. Matter* **2009,** *21*, 084203.

(14) Frisch, M. J.; Trucks, G. W.; Schlegel, H. B.; Scuseria, G. E.; Robb, M. A.; Cheeseman, J. R.; Scalmani, G.; Barone, V.; Petersson, G. A.; Nakatsuji, H.*; et al. Gaussian 09, Revision D. 01*; Gaussian, Inc., Wallingford CT, 2016.

(15) Cossi, M.; Rega, N.; Scalmani, G.; Barone, V. Energies, structures, and electronic properties of molecules in solution with the C-PCM solvation model. *J. Comput. Chem.* **2002**, *24*, 669–681.

(16) Becke, A. D. Density-functional thermochemistry. III. The role of exact exchange. *J. Chem. Phys.* **1993**, *98*, 5648–5652.

(17) Chiodo, S.; Russo, N.; Sicilia, E. LANL2DZ basis sets recontracted in the framework of density functional theory. *J. Chem. Phys.* **2006**, *125*, 104107.